Please do not adjust margins

Soft Matter

ARTICLE

Small-Angle Neutron Scattering Study of a Dense Microemulsion System formed with an Ionic Liquid†,‡

Received 00th January 20xx,
Accepted 00th January 20xx

DOI: 10.1039/x0xx00000x

www.rsc.org/

T. Kang, S. Qian, G. S. Smith, C. Do, and W. T. Heller*

Mixtures of water, octane and 1-octanol with 1-tetradecyl-3-methylimidazolium chloride (C_{14}MIM·Cl), often referred to as a surface active ionic liquid (SAIL), form water-in-oil microemulsions that have potential application as an extraction media for various metal ions. Here, we present a structural study by small-angle neutron scattering (SANS) of dense microemulsions formed by surfactant-rich mixtures of these four compounds to understand how the SAIL can be used to tune the structures and properties of the microemulsions. The SANS experiments revealed that the microemulsions formed are composed of two phases, a water-in-oil microemulsion and a bicontinuous microemulsion, which becomes the dominant phase at high surfactant concentration. In this concentration regime, the surfactant film becomes more rigid, having a higher bending modulus that results from the parallel stacking of the imidazolium ring of the SAIL. At lower surfactant concentrations, the molecular packing of the SAIL does not change with the water content of the microemulsion. The results presented here correlate well with previously observed changes in the interaction between the IL cation and metal ions (Y. Tong, L. Han and Y. Yang, *Ind. Eng. Chem. Res.*, 2012, **51**, 16438–16443), while the capacity of the microemulsion system for water remains high enough for using the system as an extraction media.

1. Introduction

Microemulsions form when two immiscible solvents, such as water and oil, are mixed in the presence of a surfactant, often with an alcohol cosurfactant. The surfactant forms a monolayer at the interface between the immiscible solvents, and the entire system self-assembles into nanoscale structures that depend on the relative concentrations of the constituents.[1] For example, water droplets dispersed in a continuous oil phase are referred to as water-in-oil microemulsions. Similarly, a bicontinuous microemulsion having interconnected channels of the two solvents can also occur at different relative concentrations of the same materials.[2] Microemulsions, which are optically transparent, are thermodynamically stable, homogeneous systems and can possess useful properties, such as low viscosity and very low interfacial tension.[1]

Microemulsions are employed as solvent media for separation and extraction of various metal ions, organic compounds, and amino acids.[3–11] The efficiency of extraction and separation processes is a function of both the solubilization of solutes and phase equilibrium of the microemulsion.[12] These properties arise from the spontaneous curvature and the elasticity of the interfacial films within the microemulsion.[13] Similarly, the structure of the microemulsion influences how solutes partition at the interface.[10,11] For example, the amino acid, tryptophan, has a high interfacial partition coefficient in a water-in-oil (isooctane) microemulsion with dioctyl sodium sulfosuccinate (AOT) when it has a low interfacial film curvature.[9] Microemulsion structures are highly sensitive to composition, temperature, and additives, which provides many ways to tune their properties for specific practical applications.

Ionic liquids (ILs) possess very low volatility and flammability, as well as high ionic conductivity and thermal

Biology and Soft Matter Division, Oak Ridge National Laboratory, Oak Ridge, TN 37831, USA. E-mail: hellerwt@ornl.gov

† Electronic Supplementary Information (ESI) available.
See DOI: 10.1039/x0xx00000x

‡ This manuscript has been authored by UT-Battelle, LLC under Contract No. DE-AC05-00OR22725 with the U.S. Department of Energy. The United States Government retains and the publisher, by accepting the article for publication, acknowledges that the United States Government retains a non-exclusive, paid-up, irrevocable, world-wide license to publish or reproduce the published form of this manuscript, or allow others to do so, for United States Government purposes. The Department of Energy will provide public access to these results of federally sponsored research in accordance with the DOE Public Access Plan (http://energy.gov/downloads/doe-public-access-plan).

Please do not adjust margins

stability,[14–16] and many researchers have investigated the behavior of ILs at surfaces and in the bulk.[17,18] ILs can also form nano-sized aggregates, such as micelles and microemulsions, where the IL serves as either the solvent or as a minor component, which have been explored as alternative solvents and extractant agents.[18–21] Specifically, ILs with a long alkyl chain moiety have been investigated as surfactants, and are often referred to as surface active ionic liquids (SAILs) because the molecules exhibit a high surface activity.[22] The self-assembly of SAILs can provide structural control for applications in chemistry, such as for creating microemulsions with dual functionality as extractant and surfactant.[23,24]

SAILs made with the well-studied imidazolium cations can be used to form microemulsions that are well-suited for extracting diverse metal ions from solution.[24,25] For example, Tong and coworkers formed microemulsions composed of hydrochloric acid solution, cyclohexane, n-hexanol, and the imidazolium-based SAIL, 1-tetradecyl-3-methylimidazolium bromide (C_{14}MIM·Br) that was highly selective for extracting gold metal ions.[24] Further, higher C_{14}MIM·Br concentrations, which formed bicontinuous microemulsions based on conductivity measurements, improved the extraction of the metal ions.[24] The work indicates that a better understanding of the relationship between composition and structure has the potential to improve the performance of SAIL-based microemulsions for this application.

Previously, the SAIL C_{14}MIM·Cl was found to form stable water-in-oil microemulsions when a small amount of water was added to octane / C_{14}MIM·Cl / 1-octanol ternary mixtures when the surfactant concentration was low.[26] The water-in-oil structure swelled in a manner consistent with its water content.[26] Here, small-angle neutron scattering (SANS) was used to characterize water / octane / C_{14}MIM·Cl / 1-octanol microemulsions in the high surfactant concentration regime, where the system is expected to form a bicontinuous microemulsion that will perform better as an extraction media. Through the use of SANS, which probes length scales from a few Å to hundreds of Å, the composition-dependent structure of the microemulsion system was revealed. The data analysis provided the physical properties of the microemulsion that are important for their use as extraction media, such as the correlation length, bending modulus and area per surfactant molecule of the bicontinuous microemulsion. The new understanding of the water / octane / C_{14}MIM·Cl / 1-octanol provided by this work can be used to guide selection of microemulsion composition for use as an extraction media.

2. Experimental section

2.1 Materials

1-tetradecyl-3-methylimidazolium chloride (C_{14}MIM·Cl; product ACM171058212; ≥ 98 %; water content < 1000 ppm), was purchased from Alfa Chemistry (Stony Brook, NY, U.S.A.). Octane (product 296988; ≥ 99 %) and deuterium oxide (D_2O; product 151882; 99.9 atom % D) were purchased from Sigma-Aldrich (St. Louis, MO, U.S.A.). 1-octanol (product A15977; 99 %) was purchased from Alfa Aesar (Haverhill, MA, U.S.A.). All chemicals were used without further purification. The sample was prepared by mixing the compounds, D_2O / surfactant (C_{14}MIM·Cl, 1-octanol) / octane at the desired molar ratios. For this study, the molar ratio of surfactant was constant, specifically [C_{14}MIM·Cl] : [1-octanol] = 1: 4.3. After mixing the components, the samples were mixed by roller mixer for 2 hours. The solutions were confirmed to be the single phases by visually inspecting the turbidity. The microemulsion phase formed was confirmed to be stable for several months. All sample preparation processes were performed at 20 °C.

Three series of sample compositions were studied, which

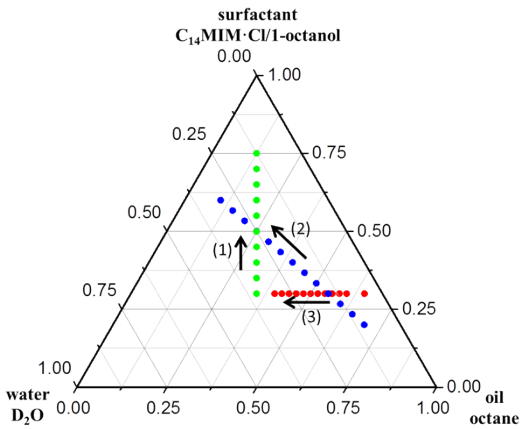

Figure 1. Ternary diagram of the mixture, D_2O / C_{14}MIM·Cl, 1-octanol / octane showing the samples studied here at a temperature of 20 °C. The molar ratio of [C_{14}MIM·Cl] : [1-octanol] = 1: 4.3 remained constant. The series of dots are the mixtures measured , and the arrows indicate the sense of increase in the three concentration series: (1) the concentration series of surfactant with equal weight percent (wt%) of water and oil, (2) the dilution series of octane solvent at constant water-to-surfactant molar ratio, and (3) the concentration series of water at constant 30 wt% surfactant. All measurements are in the single-phase region of the phase diagram, as can be seen in Fig. S1 of the ESI.

are shown in Fig. 1. Previously, we found that the mixed surfactant system, C_{14}MIM·Cl / 1-octanol, formed water-in-oil microemulsion system in non-aqueous solvent, octane, at very low surfactant concentration, 4.0 wt%.[26] The present work focuses on the high surfactant concentration region of the phase diagram where the system is expected to form a bicontinuous microemulsion. First, the concentration series of surfactant with equal weight percent (wt%) of water and oil (Fig. 1, series (1)), which is generally known to form bicontinuous microemulsion, was studied. To understand the structural change under dilution by octane solvent, the concentration series of octane solvent with a constant water-to-surfactant molar ratio was studied (Fig. 1, series (2)). Finally, the concentration series of water with a constant 30 wt% surfactant was investigated for enhancing the water solubilization of the system (Fig. 1, series (3)). Detailed compositional information, specifically the weight and volume fractions of each components, are summarized for the three series in the ESI† (Table S1).

2.2 Small-Angle Neutron Scattering (SANS)

This journal is © The Royal Society of Chemistry 20xx

Please do not adjust margins

Please do not adjust margins

SANS measurements were performed at the EQ-SANS instrument at the Spallation Neutron Source (SNS) located at Oak Ridge National Laboratory (ORNL) using 60 Hz operation.[27] The sample-to-detector distances used were 1.3 m and 4 m with the minimum neutron wavelengths set to 1.5 Å and 2.5 Å, respectively. The incident beam was collimated using a sample aperture of 10 mm. These two configurations cover a combined Q-range of 0.01 $Å^{-1} < Q < 2$ $Å^{-1}$. $Q = (4\pi/\lambda)\sin(\theta/2)$ is the magnitude of the scattering vector, where θ is the scattering angle. Data reduction to produce $I(Q)$ vs. Q was performed according to standard procedures implemented in the Mantid software,[28] and the reduced intensities were placed on an absolute scale using a calibrated porous silica standard, which is known to have a scattering intensity 450 cm^{-1} at very small Q.[29] All SANS measurements were performed at 20 °C.

2.3 SANS data analysis

SANS is a materials characterization technique that can be applied to almost any state of material. It probes density differences, specifically in the nuclear scattering length density, a measure of the interaction between the neutron and the nucleus in materials, at the nanoscale. The measured SANS intensity is given by the square of the Fourier transform of the scattering length density distribution shown in Eq. 1.

$$I(Q) \propto < |\int \rho(\vec{r}) e^{-i\vec{Q}\cdot\vec{r}} d\vec{r}|^2 > \quad (1)$$

We have analysed the scattering intensities by the combined model presented in Eq. 2, which is composed of the spherical model for the water-in-oil microemulsion and the Teubner-Strey model for the bicontinuous microemulsion with the weight of the spherical particles in the model denoted by B.

$$I(Q) = BI_{sphere}(Q) + (1-B)I_{Teubner-Strey}(Q) \quad (2)$$

In a particulate system, such as spheres, the scattering intensity is expressed by $I(Q) = n_p P(Q) S(Q)$, where n_p is the number density of particles. The form factor $P(Q)$ arises from the shape of the particle, and $S(Q)$ is the structure factor that describes interparticle spatial relationships. To describe the water-in-oil microemulsion system, the form factor of the sphere model and the hard-sphere structure factor are used.[30]

$$I_{sphere}(Q) = n_p P_{sphere}(Q) S_{hard-sphere}(Q),$$

$$n_p P_{sphere}(Q) = \frac{\emptyset_1}{4\pi R^3/3}(\rho_{sphere} - \rho_{solvent})^2$$

$$\int_0^\infty \left\{\frac{4\pi R^3(\sin(QR) - QR\cos(QR))}{(QR)^3}\right\}^2 f(r)dr. \quad (3)$$

$\emptyset_1$ is the volume fraction of sphere. The scattering length density (SLD) contrast between spherical particle and solvent is defined as $\rho_{sphere} - \rho_{solvent}$. The polydispersity of the sphere radius is described by the Schulz distribution $f(r)$,

$$f(r) = \left(\frac{z+1}{\bar{r}}\right)^{z+1} r^z \exp\left(-\frac{z+1}{\bar{r}}r\right)\frac{1}{\Gamma(z+1)}, \quad z > -1. \quad (4)$$

Here, $\bar{r}$ and $\Gamma(z)$ are the mean radius and the Gamma function respectively.[31] The value of z is related to the polydispersity $(\overline{r^2} - \bar{r}^2)^{1/2}/\bar{r} = (z+1)^{-1/2}$ by the root-mean-square deviation from the mean radius.[31]

For the bicontinuous microemulsion system, the Teubner-Strey model is used, which has two characteristic lengths: the correlation length (ξ) and the repeat distance (d) of water and oil phase.[32,33]

$$I_{Teubner-Strey}(Q) = \emptyset_2 \Delta\rho^2 \frac{8\pi\xi^3}{\left\{1 + \left(\frac{2\pi\xi}{d}\right)^2\right\}^2 + \left\{-2\xi^2\left(\frac{2\pi\xi}{d}\right)^2 + 2\xi^2\right\}Q^2 + \xi^4 Q^4} + \frac{c}{Q^4}\exp\left(-Q^2T^2\right) \quad (5)$$

$\emptyset_2$ is the volume fraction of the polar phase in the system, and T is the thickness of surfactant film. The SLD difference between the polar and non-polar phase is defined as Δρ. The second term of the Teubner-Strey equation describes Porod-like limiting behaviour in the high Q-region. The coefficient c is related to the volume fraction of surfactant, scattering length density contrast, and the effective film thickness ($c = 2\pi\Delta\rho^2 \emptyset_{surf}\frac{1}{\sqrt{2\pi}T}$). The scattering intensity decreases in proportion to Q^{-4} for the high Q-region as a result of an abrupt change of the scattering length density, as is the case for the interface between the polar and non-polar components in a microemulsion, while the exponential term leads to a steeper decay than Q^{-4} decay.[33]

3. Results and Discussion

The specific systematic composition series investigated by small-angle neutron scattering (SANS) are presented in the ternary diagram shown in Fig. 1. The surfactant concentration series possessing equal weight percent (wt%) of water and oil corresponds to the curve labelled (1). SANS data collected in this series are presented in Fig. 2. As can be seen in Fig. 2, the data display a peak that shifts to higher Q, corresponding to smaller distances, with increasing surfactant wt%. Overall, the data are well-fit by the model shown in Eq. 2, and the parameters obtained by the fitting are summarized in Table S2 of the ESI†. For the water-in-oil microemulsion, the polar phase, which is spherical particle portion of the model, is composed of D_2O and the head group of the mixed surfactant, C_{14}MIM·Cl / 1-octanol. Therefore, the scattering length density (SLD) of the sphere was estimated from the composition and was fixed for the fitting. Similarly, the solvent consists of the alkyl chain of the mixed surfactant, C_{14}MIM·Cl / 1-octanol, and octane, and it was possible to fix the SLD based on the material composition to be -0.5×10^{-6} $Å^{-2}$. An additional constraint requiring that the SLD difference between the polar and non-polar phase in the Teubner-Strey model ($\Delta\rho$) have the same value as the SLD difference between the sphere and solvent (

Please do not adjust margins

Please do not adjust margins

$\rho_{sphere} - \rho_{solvent}$) in the sphere model was also applied. As Table S2 shows, the size of sphere and its weight in the model, *B*, decreases with increasing surfactant concentration, which indicates that the bicontinuous microemulsion phase becomes dominant at the highest surfactant concentrations. Ultimately, for surfactant concentrations from 55 wt% to 75 wt%, the SANS profiles are well-fit using only the $I_{Teubner-Strey}(Q)$ model. These curves are shown in Fig. 2b.

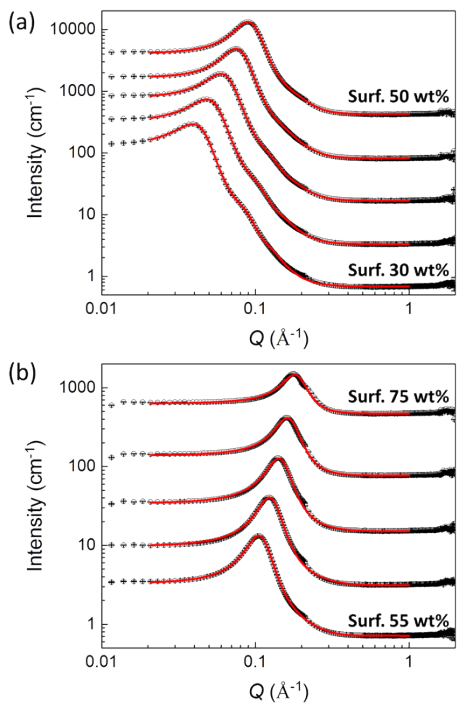

Fig. 2 Scattering intensities in terms of surfactant concentration (a) from 30 wt% to 50 wt% and (b) from 55 wt% to 75 wt% (Δ = 5 wt%). Fitting curves obtained by (a) the combined model and (b) the only Teubner-Strey model ($I_{Teubner-Strey}(Q)$) are indicated by red line. With the exception of the data sets collected for 30 wt% and 55 wt% surfactant, the data have been offset by multiplicative constants for clarify.

The fitting results of the Teubner-Strey model can be related to physical properties of the bicontinuous microemulsion. The amphiphilic factor, $f_a = \frac{1-(2\pi\xi/d)^2}{1+(2\pi\xi/d)^2}$, is a measure of the amphiphilic strength of the system, which dictates the microstructure.[34,35] For example, when f_a is between -0.70 and -0.90, the system is a well-structured bicontinuous microemulsion.[34] Similarly, values of f_a close to -1.0 indicate a lamellar phase.[35] For $f_a = 0$, it corresponds to the Lifshitz Line, which indicates the disappearance of the structure peak.[34] Disorder line of microemulsion system corresponds to $f_a = 1$ and indicates looseness of its quasiperiodic ordering.[34] The renormalized bending modulus can be derived from the two characteristic lengths obtained from the data fitting, specifically the correlation length ξ and the repeat distance d, according to the relation $\kappa_{SANS} = \frac{5\sqrt{3}}{64} k_B T \frac{2\pi\xi}{d}$, where k_B and T are Boltzmann's constant and the absolute temperature, respectively.[34,36] The renomalized bending modulus describes fluctuation of surfactant film in the characteristic length scale of the bicontinuous microemulsion.[34,36] The characteristic length (ξ) is also used to determine the surface area per volume. The surface area per volume, $\frac{S}{V} = \frac{4\emptyset_{water}\emptyset_{oil}}{\xi}$, which is a function of the volume fractions of water and oil,[33] can be used to derive the specific area per surfactant head group, $A_s = \frac{v_s}{\emptyset_{surfactant}}\left(\frac{S}{V}\right)$.[37] For the samples studied here, the total volume of surfactant v_s is

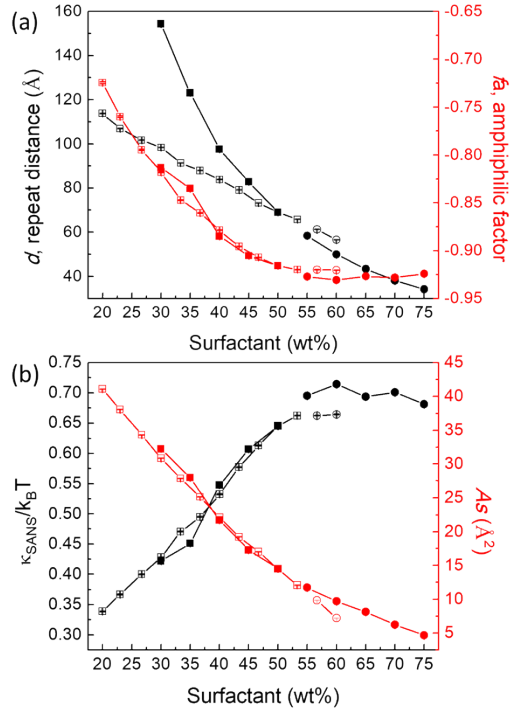

Fig. 3 Values derived from the Teubner-Strey model (a) repeat distance (d, black dot) and amphiphilic factor (f_a, red dot), (b) bending modulus (κSANS/k_BT, black dot) and specific area per surfactant head group (A_s, red dot) in terms of the surfactant concentration. Closed dot and open dot represent (1) the concentration series of surfactant with equal weight percent (wt%) of water and oil and (2) the dilution series of octane solvent at constant water-to-surfactant molar ratio respectively. Square and circle dot indicate results from the combined model and only the Teubner-Strey model respectively.

estimated as 1530 Å^3 by total volume of a C_{14}MIM·Cl and 4.3 1-octanol molecules. The volume of surfactant molecules are calculated by the volume of hydrophilic head group and alkyl chain group. Crystallographically determined diameter of imidazolium ring of C_{14}MIM·Cl is ~5.4 Å,[38] and a hydroxyl group (OH) of 1-octanol is assumed as a sphere with a size of ~1 Å. Therefore, the volume of surfactant head group is ~85 Å^3. The volume of alkyl chain group was estimated according to Tanford's relation, $27.4 + 26.9 * n_c\ (\text{Å}^3)$, where n_c is the number of carbon atoms.[39]

The microemulsion properties provided by the data fitting of the (1) series of samples are presented in Fig. 3 (closed dots) and Table S3. With increasing surfactant concentration, the repeat distance decreases. Concurrently, the value of f_a decreases from -0.81 to -0.93, where it saturates at ~55 wt% surfactant, indicating that the bicontinuous microemulsion transitions to the lamelar phase at ~55 wt%.

This journal is © The Royal Society of Chemistry 20xx

Please do not adjust margins

Please do not adjust margins

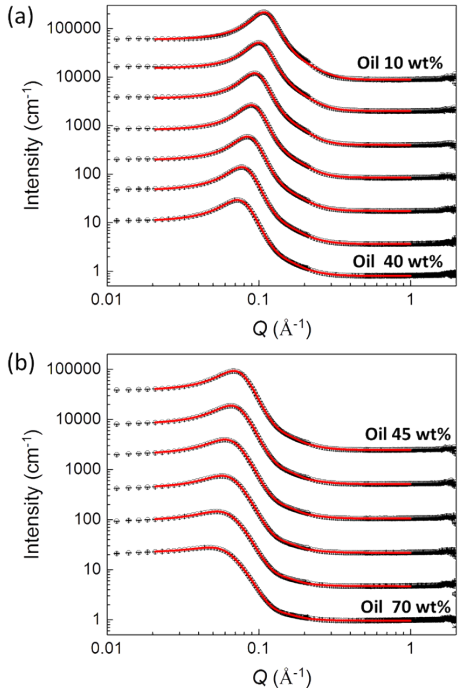

Fig. 4 Scattering intensities in terms of oil concentration (a) from 10 wt% to 40 wt% and (b) from 45 wt% to 70 wt% (Δ = 5 wt%). Fitting curves obtained by the combined model (20 wt% - 70 wt%) and the only Teubner-Strey model ($I_{Teubner-Strey}(Q)$) (10 wt% - 15 wt%) are indicated by red line. With the exception of the SANS data collected for 40 wt% and 70 wt% surfactant, the SANS data have been offset by multiplicative constants for clarity.

The bending modulus also increases with increasing surfactant concentration and plateaus at a similar surfactant concentration. Such a trend has been observed previously for the bicontinuous microemulsion system of D_2O / n-decyltetraoxyethylene / hexane, the bending modulus obtained by SANS spectra increased ~0.35 to ~0.45 when the surfactant volume fraction increases from ~0.07 to ~0.09.[36] The value of A_s, however, monotonically decreases throughout the range of concentrations studied. We can estimate the area of surfactant as ~23 Å^2 from the previously determined volume of surfactant head group, ~85 Å^3.[38] The final value obtained for A_s around 40 wt% is similar to the estimated specific area. The results suggest that the packing of surfactant molecules increases along with the surface layer rigidity as the concentration increases. Such variation may be attributed to the exclusion of 1-octanol, which leaves the imidazolium rings stacked in a parallel arrangement. And the molecular geometry of the imidazolium rings is strongly related with the interaction between the IL and hydrophilic solutes, such as metal ions. By the infrared spectroscopic measurements, Tong and coworkers found that extraction of gold metal ions is induced by a strong interaction between the cationic imidazolium ring of C_{14}MIM·Br and the tetrachloroaurate anion, $AuCl_4^-$ in the microsmulsion system composed of hydrochloric acid solution / cyclohexane / n-hexanol / C_{14}MIM·Br.[24] Therefore, the extraction capacity of the microemulsion system is strongly related with the arrangement of the IL imidazolium ring and physical properties of the surfactant film, and the present work indicates how to control this feature of the system.

The concentration series of octane at a constant water-to-surfactant molar ratio, series (2) of Fig. 1, was also studied by SANS to understand the structural change under dilution by solvent. The SANS data are presented in Fig. 4. When the system is diluted with octane, i.e. the concentration of oil increases, the peak shifts to smaller values of *Q*, which corresponds to larger distances. Overall, the data are well-fit by the combined model shown in Eq. 2, and the fitting results are summarized in terms of the surfactant concentration in Table S4 for easy comparison with the other series of samples studied. Much like series (1), the size of spheres and the fraction of the water-in-oil microemulsion phase decreases with increasing the surfactant concentration. For the highest surfactant concentrations measured, 56.7 wt% and 60.0 wt%, the SANS profile are well-fit using only the Teubner-Strey model. Similarly, in the case of 20 wt% surfactant, the porod limit term for high *Q*-region of the Teubner-Strey model in Eq. 5 was not employed due to the high incoherent scattering background that resulted from the large amount of hydrogen in the sample.

For the bicontinuous microemulsion system, the physical parameters derived from the Teubner-Strey model fitting results for the (2) series of samples are summarized as a function of the surfactant concentration in Fig. 3 (open dots) and Table S3. As was observed for series (1), the repeat distance decreases with increasing surfactant wt%, and the amphiphilic factor decreases from -0.72 to -0.92 at ~55 wt%, where it saturates. Below this saturation concentration, the repeat distances of the samples in series (2) (open dots) are smaller than those of the samples in series (1) (closed dots), which can be attributed to the lower water-to-oil ratio. Taken together, the (1) and (2) series of samples indicate that the bicontinuous microemulsion gives way to a lamellar phase at ~55 wt% surfactant. As shown in Fig 3b (open dots), the value of κ_{SANS}/k_BT increases and saturates at the same surfactant concentration. And the value of *As* decreases with increasing surfactant concentration. It represents that the surfactant film becomes more rigid with increasing surfactant concentration as a result of the parallel stacking of the imidazolium ring of the SAIL similarly with the (1) series (Fig. 3b, closed dots). A strong interaction between the IL cation and metal chloride anions, such as $AuCl_4^-$, exists that makes it possible to extract metal ions from hydrochloric acid solution.[24] Again, the present results demonstrate how to tune the IL molecular arrangement and elasticity of surfactant film to improve the microemulsion's extraction capacity.

Please do not adjust margins

Please do not adjust margins

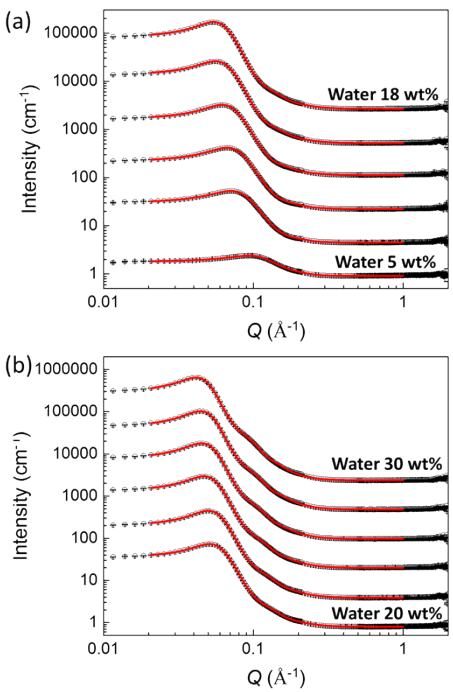

Fig. 5 Scattering intensities in terms of water contents (a) from 5 wt% to 18 wt% and (b) from 20 wt% to 30 wt%. Fitting curves obtained by the combined model are indicated by red line. The SANS data, with the exception of those containing 5 wt% and 20 wt% water are offset by multiplicative constants for clarify.

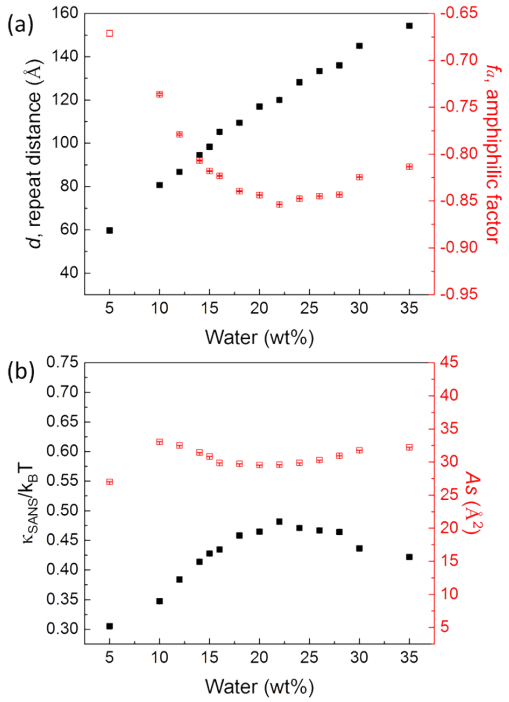

Fig. 6 Values derived from the Teubner-Strey model (a) repeat distance (d, closed black dot) and amphiphilic factor (f_a, open red dot), (b) bending modulus (κ_{SANS}/k_BT, closed black dot) and specific area per surfactant head group (A_S, open red dot) n terms of the water content.

The final series of samples studied, which is the curve labelled (3) in Fig. 1, was a water concentration series performed at a constant 30 wt% surfactant to determine the water solubilisation capacity of the dense microemulsion system. With increasing water amounts, the peak shifts to the smaller *Q*, indicating larger structures. All of the SANS data, which are presented in Fig. 5, are well-fit with the combined model shown in Eq. 2. The fitting results are summarized in Table S5, and show that the size of spheres of the water-in-oil microemulsion phase increases with the water concentration. The results of 15 and 35 wt% water are the one from series (2) and (1), respectively (details in ESI†). The physical properties of the bicontinuous microemulsion derived from the Teubner-Strey model fitting results are presented in Fig. 6 and Table S3, series (3), as a function of water concentration. The repeat distance increases with increasing water amounts, and f_a ranges from -0.70 to -0.85 except for the 5 wt% water sample, which indicates that the system is a well-structured bicontinuous microemulsion for most of the mixtures in the series (3). Further, the values of κ_{SANS}/k_BT are essentially constant for water contents above 20 wt%, while A_s is essentially independent of water content compared to series (1) and (2). For the 5 wt% water sample, f_a is greater than -0.70, which is the maximum value representing well-structured bicontinuous microemulsion and the values found for the remainder of series (3). Interestingly, the bending modulus for this series of samples is generally lower than the other series of samples measured, even at high water content. It indicates that the molecular geometry of the ionic liquid does not change at a broad range of water contents sustaining well-structured bicontinuous microemulsion, while the both size of the water-in-oil microemulsion and bicontinuous microemulsion increase with increasing water contents. These results confirm the water solubilization capacity of the system, which is important for extracting metal ions from aqueous solution.[5]

4. Conclusions

The structure of dense microemulsion system with the SAIL C_{14}MIM·Cl, has been investigated as a function of composition by SANS. With increasing the surfactant concentration, the bicontinuous microemulsion becomes dominant, and the structural transition from bicontinuous microemulsion to lamellar phase is found at ~55 wt% surfactant concentration. For the high surfactant concentration region, the surfactant film becomes more rigid and ordered, and parallel stacking of the imidazolium ring of the C_{14}MIM·Cl is expected for the ordered phase. At lower surfactant concentration, 30 wt%, the both size of the water-in-oil microemulsion and bicontinuous microemulsion increase with increasing water content, and the molecular geometry of the ionic liquid does not change in terms of water amounts. The present results demonstrate that the structure and physical properties of the microemulsion can

This journal is © The Royal Society of Chemistry 20xx

Please do not adjust margins

Please do not adjust margins

be tuned by varying its composition. An optimal extraction of metal ions can be achieved by understanding structure deformation of microemulsion with varying compositions. Specially, tuning of IL molecular geometry in terms of compositions is useful to control the interaction between IL cation and metal ions that makes it possible to extract metal ions.[24] The present work also indicates that this microemulsion system which has a high enough water solubility to make it useful as an extraction media of metal ions in aqueous solution.

Acknowledgements

The Research at Oak Ridge National Laboratory's Spallation Neutron Source was sponsored by the Scientific User Facilities Division, Office of Basic Energy Sciences, U. S. Department of Energy. Research sponsored by the Laboratory Directed Research and Development Program (LDRD-7641) of Oak Ridge National Laboratory, managed by UT-Battelle, LLC, for the U. S. Department of Energy.

References

1 P. G. De Gennes and C. Taupin, *J. Phys. Chem.*, 1982, **86**, 2294–2304.
2 D. Andelman, M. E. Cates, D. Roux and S. A. Safran, *J. Chem. Phys.*, 1987, **87**, 7229–7241.
3 M. Ismael and C. Tondre, *J. Memb. Sci.*, 1992, **72**, 181–188.
4 D. He, C. Yang, M. Ma, L. Zhuang, X. Chen and S. Chen, *Colloids Surfaces A Physicochem. Eng. Asp.*, 2004, **232**, 39–47.
5 E. Paatero, J. Sjöblom and S. . Datta, *J. Colloid Interface Sci.*, 1990, **138**, 388–396.
6 T. N. Castro Dantas, K. R. Oliveira, A. A. Dantas Neto and M. C. P. A. Moura, *Water Res.*, 2009, **43**, 1464–1470.
7 H. Naganawa, H. Suzuki and S. Tachimori, *Phys. Chem. Chem. Phys.*, 2000, **2**, 3247–3253.
8 T. N. Castro Dantas, M. H. de Lucena Neto, A. A. Dantas Neto, M. C. P. Alencar Moura and E. L. Barros Neto, *Ind. Eng. Chem. Res.*, 2005, **44**, 6784–6788.
9 E. V. Brejza and E. S. Perez de Ortiz, *J. Colloid Interface Sci.*, 2000, **227**, 244–246.
10 P. D. I. Fletcher, *J. Chem. Soc. Faraday Trans. 1 Phys. Chem. Condens. Phases*, 1986, **82**, 2651.
11 E. B. Leodidis, A. S. Bommarius and T. A. Hatton, *J. Phys. Chem.*, 1991, **95**, 5943–5956.
12 S. P. Moulik and B. K. Paul, *Adv. Colloid Interface Sci.*, 1998, **78**, 99–195.
13 R. Leung and D. O. Shah, *J. Colloid Interface Sci.*, 1987, **120**, 320–329.
14 P. Bonhôte, A.-P. Dias, N. Papageorgiou, K. Kalyanasundaram and M. Grätzel, *Inorg. Chem.*, 1996, **35**, 1168–1178.
15 J. G. Huddleston, A. E. Visser, W. M. Reichert, H. D. Willauer, G. A. Broker and R. D. Rogers, *Green Chem.*, 2001, **3**, 156–164.
16 M. Ahrenberg, M. Brinckmann, J. W. P. Schmelzer, M. Beck, C. Schmidt, O. Keßler, U. Kragl, S. P. Verevkin and C. Schick, *Phys. Chem. Chem. Phys.*, 2014, **16**, 2971.
17 Y. Jeon, D. Vaknin, W. Bu, J. Sung, Y. Ouchi, W. Sung and D. Kim, *Phys. Rev. Lett.*, 2012, **108**, 55502.
18 A. Triolo, O. Russina, H.-J. Bleif and E. Di Cola, *J. Phys. Chem. B*, 2007, **111**, 4641–4644.
19 J. N. A. Canongia Lopes and A. A. H. Pádua, *J. Phys. Chem. B*, 2006, **110**, 3330–3335.
20 R. Atkin, S. M. C. Bobillier and G. G. Warr, *J. Phys. Chem. B*, 2010, **114**, 1350–1360.
21 Y. Gao, L. Hilfert, A. Voigt and K. Sundmacher, *J. Phys. Chem. B*, 2008, **112**, 3711–3719.
22 O. A. El Seoud, P. A. R. Pires, T. Abdel-Moghny and E. L. Bastos, *J. Colloid Interface Sci.*, 2007, **313**, 296–304.
23 O. Zech, S. Thomaier, P. Bauduin, T. Rück, D. Touraud and W. Kunz, *J. Phys. Chem. B*, 2009, **113**, 465–473.
24 Y. Tong, L. Han and Y. Yang, *Ind. Eng. Chem. Res.*, 2012, **51**, 16438–16443.
25 J. A. Whitehead, J. Zhang, N. Pereira, A. McCluskey and G. A. Lawrance, *Hydrometallurgy*, 2007, **88**, 109–120.
26 T. H. Kang, Y. Jeon and M. W. Kim, *Phys. Chem. Chem. Phys.*, 2015, **17**, 27833–27839.
27 J. K. Zhao, C. Y. Gao and D. Liu, *J. Appl. Crystallogr.*, 2010, **43**, 1068–1077.
28 O. Arnold, J. C. Bilheux, J. M. Borreguero, A. Buts, S. I. Campbell, L. Chapon, M. Doucet, N. Draper, R. Ferraz Leal, M. A. Gigg, V. E. Lynch, A. Markvardsen, D. J. Mikkelson, R. L. Mikkelson, R. Miller, K. Palmen, P. Parker, G. Passos, T. G. Perring, P. F. Peterson, S. Ren, M. A. Reuter, A. T. Savici, J. W. Taylor, R. J. Taylor, R. Tolchenov, W. Zhou and J. Zikovsky, *Nucl. Instruments Methods Phys. Res. Sect. A Accel. Spectrometers, Detect. Assoc. Equip.*, 2014, **764**, 156–166.
29 G. D. Wignall and F. S. Bates, *J. Appl. Crystallogr.*, 1987, **20**, 28–40.
30 A. Guinier and G. Fournet, *Small-Angle Scattering of X-Rays*, John Wiley and Sons, New York, 1955.
31 M. Kotlarchyk and S. Chen, *J. Chem. Phys.*, 1983, **79**, 2461–2469.
32 R. Strey, J. Winkler and L. Magid, *J. Phys. Chem.*, 1991, **95**, 7502–7507.
33 K. -V. Schubert and R. Strey, *J. Chem. Phys.*, 1991, **95**, 8532–8545.
34 S. Engelskirchen, N. Elsner, T. Sottmann and R. Strey, *J. Colloid Interface Sci.*, 2007, **312**, 114–121.
35 K. -V. Schubert, R. Strey, S. R. Kline and E. W. Kaler, *J. Chem. Phys.*, 1994, **101**, 5343–5355.
36 S. Maccarrone, D. V. Byelov, T. Auth, J. Allgaier, H. Frielinghaus, G. Gompper and D. Richter, *J. Phys. Chem. B*, 2013, **117**, 5623–5632.
37 D. G. Hayes, J. A. Gomez del Rio, R. Ye, V. S. Urban, S. V. Pingali and H. M. O'Neill, *Langmuir*, 2015, **31**, 1901–1910.

Please do not adjust margins

Please do not adjust margins

38 T. H. Kang, M. W. Kim and Y. Jeon, *J. Phys. Chem. C*, 2013, **117**, 14332–14337.
39 C. Tanford, *J. Phys. Chem.*, 1972, **76**, 3020–3024.

This journal is © The Royal Society of Chemistry 20xx

Please do not adjust margins